2014

Bone growth following demineralized bone matrix implantation requires angiogenesis

BOSTON UNIVERSITY

SCHOOL OF MEDICINE

Thesis

BONE GROWTH FOLLOWING DEMINERALIZED BONE MATRIX IMPLANTATION REQUIRES ANGIOGENESIS

by

STEPHANIE LAM

B.S., University of Southern California, 2012

Submitted in partial fulfillment of the

requirements for the degree of

Master of Science

2014

Approved by

First Reader

Louis C. Gerstenfeld, Ph.D.
Professor of Orthopaedic Surgery

Second Reader

Beth Bragdon, Ph.D.
Postdoctoral Research Fellow

DEDICATION

I would like to dedicate this work to my parents, who have always supported my educational endeavors.

ACKNOWLEDGEMENTS

I would like to thank Dr. Louis C. Gerstenfeld and Dr. Beth Bragdon for guidance throughout this project, and for serving as readers for this thesis. I have learned many more tricks and methods around the laboratory that serve as wonderful transferrable skills in the science world as a result of their training.

BONE GROWTH FOLLOWING DEMINERALIZED BONE MATRIX IMPLANTATION REQUIRES ANGIOGENESIS

STEPHANIE LAM

ABSTRACT

Angiogenesis is required for endochondral ossification during development and fracture healing; however the exact mechanisms and temporal relationship between the two processes remains unclear. In this study, we utilize an *in vivo* model of endochondral ossification in mice by implanting demineralized bone matrix (DBM) proximal to the femur to induce ectopic bone formation. TNP-470, a drug known to be anti-angiogenic, was used to inhibit vascularization during the time course of *de novo* bone formation in order to define the role of angiogenesis during the chondrogenic phase of endochondral bone formation. Day 2, day 8, and day 16 post-surgery were selected time points to represent pre-chondrogenic, chondrogenic, and bone mineralization stages, respectively. Plain x-ray and micro-CT analysis showed that inhibition of angiogenesis led to decreased mineralized tissue formation. Inhibited angiogenesis was confirmed with qRT-PCR. Most striking, however, is that while stem cells are recruited and committed to the chondrogenic lineage, subsequent chondrogenesis failed to progress based on the failure of *Sox5* and *Sox6* expression, which directs chondrocyte commitment. This expands the role for angiogenesis to a much earlier stage than currently thought and places the necessity of angiogenesis very early in the endochondral ossification process.

TABLE OF CONTENTS

LIST OF TABLES

LIST OF FIGURES

LIST OF ABBREVIATIONS

α-SMA.....alpha smooth muscle actin

ACAN.....aggrecan

BMP.....bone morphogenetic protein

BMP2.....bone morphogenetic protein 2

BMPRI.....bone morphogenetic protein receptor type 1

BMPRII.....bone morphogenetic protein receptor type 2

cDNA.....complementary deoxyribonucleic acid

COL10A1.....collagen type X alpha 1

COL2A1.....collagen type II alpha 1

DAG.....diacylglycerol

DBM.....demineralized bone matrix

DMP1.....dentin matrix protein 1

dNTP.....deoxyribonucleotide triphosphate

ERK.....extracellular signal regulated kinases

FDA.....Food and Drug Administration

GDF5.....growth differentiation factor 5

His.....Histidine

IP_3.....inositol triphosphate

kVp.....peak kilovoltage

MEK.....mitogen activated protein kinase

METAP-2.....methionine aminopeptidase-2

$MgCl_2$.....magnesium chloride

micro-CT.....micro-computed tomography

mRNA.....messenger ribonucleic acid

N-Cadherin.....neural cadherin

Nanog.....nanog homeobox

NCAM1.....neural cell adhesion molecule 1

NSAID.....non-steroidal anti-inflammatory drug

PAX7.....paired box 7

PBS.....phosphate buffered saline

PCR.....polymerase chain reaction

PECAM1.....platelet endothelial cell adhesion molecule 1

PFA.....paraformaldehyde

PKC..... .....protein kinase C

PRX1.....paired related homeobox protein 1

qPCR.....quantitative polymerase chain reaction

qRT-PCR.....quantitative real-time polymerase chain reaction

rhBMP-2.....recombinant human bone morphogenetic protein 2

RNA.....ribonucleic acid

RNase.....ribonuclease

RT.....real time

RUNX2.....runt-related transcription factor 2

SFLT1.....soluble fms-like tyrosine kinase 1

SOX2.....sex determining region Y-box 2

SOX5.....sex determining region Y-box 5

SOX6.....sex determining region Y-box 6

SOX9.....sex determining region Y-box 9

SRY.....sex determining region Y

TGF-ß.....transforming growth factor ß

TRAP5B.....tartarate-resistant acid phosphatase 5b

VE-cadherin.....vascular endothelial cadherin

VEGF.....vascular endothelial growth factor

VEGFR.....vascular endothelial growth factor receptor

INTRODUCTION

Each year, approximately 6 million people in the United States experience bone fractures, 300,000 of which inefficiently heal or are unable to fully recover from injury ("Physical Fields", 2002, para. 1). Bone fractures are attributable to phenomenon ranging anywhere from rigorous sports to vitamin deficiencies, hormonal imbalances, and normal aging (Lips, 2001). Bone fractures heal via endochondral ossification, which utilizes a cartilage model, and intramembranous ossification, which does not require cartilage. While both processes are involved in bone formation during development and in repairing bones after injury, endochondral ossification is required for axial and appendicular long and short bone formation (Mescher, 2010, p.129). Thus, thoroughly understanding the molecular mechanisms of endochondral ossification is critical to gaining insight into bone development and into the development of therapies for fracture healing.

Endochondral Ossificiation

Endochondral ossification is responsible for the development of most bones and begins with hyaline cartilage that is gradually replaced by bone. Hyaline cartilage mainly consists of type II collagen, but type VI collagen and type IX collagen are also present. In addition to its vital role in endochondral ossification, hyaline cartilage can be found in the joints, nose, bronchi, trachea, larynx, and ventral ends of the ribs (Mescher, 2010, p. 114).

The endochondral ossification process starts with mesenchymal stem cells that condense to form cartilage. While markers specific to mesenchymal stem cells are poorly understood, transcription factors such as sex determining region Y (SRY)-box 2 (*Sox2*) and nanog homeobox (*Nanog*) have been suggested to be specifically expressed in all stem cells. Thus, they can be used as a means to measure mesenchymal stem cell recruitment (Park et al., 2012).

SRY-box 9 (*Sox9*) is a transcription factor that is considered to be the earliest marker of chondrogenesis. *Sox9* expression initiates stem cell commitment to the chondrocyte lineage (Kondo et al., 2013). Further, *Sox9* activation leads to the activation of other chondrogenic transcription factors, SRY-box 5 (*Sox5*) and SRY-box 6 (*Sox6*) that, together, regulate the progression of chondrocyte differentiation. There is, however, redundancy between *Sox5* and *Sox6*; expression of just one of these transcription factors was enough to avoid severe skeletal developmental abnormalities. Yet, *Sox9* remains absolutely necessary for chondrogenesis, as inhibition of *Sox9* has been shown to inhibit pre-cartilage condensation and all subsequent skeletal mechanisms (Akiyama & Lefebvre, 2011).

The commitment of stem cells to chondrocytes leads to condensation, a stage in which mesenchymal cells condense into clusters that will eventually fully differentiate into chondrocytes. Neural cadherin (*N-cadherin*) and neural cell adhesion molecule 1 (*Ncam1*) are two genes particularly critical to the condensation process; N-CADHERIN is responsible for initiating condensation, while NCAM1 is vital to the maintenance of condensation (Gilbert, 2000). Condensation of mesenchymal cells leads to

chondrogenesis, or cartilage formation, by chondrocytes at the epiphyseal plate (Mackie, 2008).

Collagen type II alpha 1 (*Col2a1*) is a gene for type II collagen and is considered one of the earliest chondrogenesis markers (Leung et al., 2011). Aggrecan (*Acan*) is downstream of *Col2a1* in the chondrogenic process (Weber et al., 2013) and codes for cartilage proteoglycan (Han & Lefebvre, 2008). As ossification begins, the cartilage model is invaded by a mixture of cells (Mackie, 2008). A bone collar is formed by osteoblasts of the perichondrium and plays a role in preventing the transport of oxygen and nutrients to the underlying cartilage, which leads to the resorption of cartilage and, ultimately, programed cell death. Chondrocytes produce alkaline phosphatase and hypertrophy, causing the enlargement of lacunae, compression of the matrix, and calcification of the matrix (Mescher, 2010, p.129) (Figure 1). Collagen type X alpha 1 (*Col10a1*) codes for these hypertrophic chondrocytes (Smits et al., 2001). Vascularization of the tissue occurs through perforations in the bone collar. Osteoprogenitors come into the bone via these vessels and differentiate into osteoblasts, which produce woven bone over the calcified cartilage matrix. The woven bone eventually remodels into compact bone, and ultimately, the last of the mineralized cartilage matrix is replaced by bone (Mescher, 2010, p.130).

A second mechanism by which fracture healing may occur is intramembranous ossification. In intramembranous ossification, cells of the mesenchymal condensation layer differentiate into osteoblasts that lay down an osteoid matrix; calcification ensues, causing encapsulation of some osteoblasts that eventually become osteocytes. Then, the

connective tissue is vascularized, some mesenchymal cells differentiate into bone marrow, and the ossification centers radially expand until they fuse with one another.

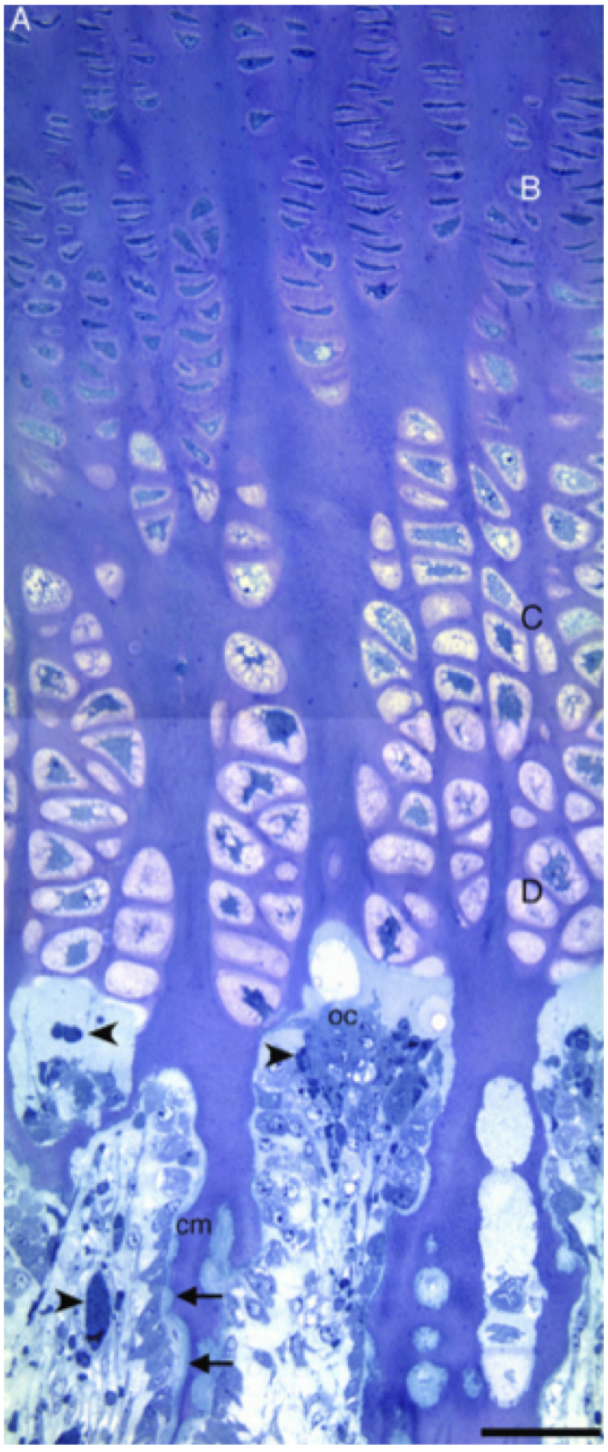

Figure 1. Light micrograph of endochondral ossification. Arrowheads point to vascularization, oc denotes osteoclasts, arrows point to deposition of bone matrix, and cm denotes cartilage matrix remnants. (A) Epiphyseal growth plate. (B) Chondrocyte proliferation.(C) Hypertrophic chondrocytes. (D) Enlargement of lacunae. Figure taken from Mackie et al., 2008.

Intramembranous ossification primarily takes place during the condensation of embryonic mesenchymal tissue and is responsible for the formation of the skull, the mandible, and the maxilla (Mescher, 2010, p.129).

Mechanism of Bone Formation

Bone formation is induced by growth factors known as bone morphogenetic proteins (BMPs). Bone morphogenetic protein 2 (BMP2), a ligand of the transforming growth factor ß (TGF-ß) superfamily, acts by binding

to BMP receptor type II (BMPRII), a serine-threonine receptor kinase. It then recruits and phosphorylates BMP receptor type I (BMPRI). In turn, BMPRI phosphorylates SMAD1, SMAD5, and SMAD8, which complex with co-SMAD4 to undergo translocation to the nucleus, where they interact with transcription factors and regulate gene expression. An example of such a transcription factor is Runt-related transcription factor 2 (*Runx2*), which is involved with osteoblast differentiation (Chen et al., 2004). An antagonist to BMP signaling is NOGGIN (Gobeske et al., 2009), which has been shown to decrease both osteoblast action and differentiation (Devlin et al., 2003). BMP2 is essential for bone repair and formation. A study on mice showed that those unable to produce BMP2 experienced spontaneous fractures and were unable to recover from them, despite other osteogenic genes being present (Tsuji et al., 2006). In fact, when a mouse model lacking proper expression of BMPRII was created by truncation of the C-terminal of *Bmpr2*, the mice showed smaller embryos, delayed bone mineralization, and slower skeletal development overall (Yang et al., 2010).

There are two main types of cells associated with bone formation: osteoblasts/osteocytes and osteoclasts. Osteoblasts arise from the differentiation of multipotent mesenchymal stem cells, and their primary function is the formation of new bone (Harada & Rodan, 2003). *Osterix* (Lee et al., 2003) and *Osteocalcin* (Ducy & Karsenty, 1995) are both markers for osteoblasts. Osteoblasts that become embedded within their own secretions and mineralized bone become terminally differentiated and are called osteocytes. Their roles are involved in bone networks for exchange of nutrients and bone turnover (Aarden et al., 1994). Dentin matrix protein 1 (*Dmp1*) is a gene that is

expressed by osteocytes of lamellar and woven bone (Kashima et al., 2013). On the other hand, bone resorption is the function of osteoclasts, which are derived from monocytes (Fujikawa et al., 1996). Tartrate-resistant acid phosphatase 5b (*Trap5b*) is a marker whose expression parallels the number of osteoclasts present (Henriksen et al., 2007).

The first type of bone tissue that appears in both development and fracture repair is woven bone, which appears as random collagen fibers and is low in mineral content. Woven bone is eventually replaced by lamellar bone containing multiple sheets of calcified matrix or lamellae. These lamellae are organized around a canal containing loose connective tissue, vascularization, and nerves called an osteon, creating the haversian system. Each lamella contains type I collagen fibers that are important for the strength and durability of compact bone. Bone remodeling is a process in which bone formation and resorption occur in a coupled manner and is a continuous, homeostatic process that replaces old bone with new bone (Mescher, 2010, p.125).

Vascularization in Endochondral Ossification: Clues in Bone Healing

Vascular endothelial growth factor (VEGF) is a master regulator of hematopoiesis and blood vessel development and is thus crucial to angiogenesis (Gerber et al., 2002). VEGF ligands, five of which have been identified, bind to one of three tyrosine kinase VEGF receptors (VEGFR) that have been identified: VEGFR-1, VEGFR-2, and VEGFR-3. VEGFR-2 is responsible for endothelial cell growth, and the ligand VEGF-A has been found to play a critical role in normal vascular development. When activated by extracellular VEGF-A binding, VEGFR-2 dimerizes and undergoes auto-phosphorylation

of its intracellular tyrosine residues. Intracellular signaling leads to eventual hydrolysis of phosphatidylinositol 4,5-bisphosphate by phospholipase C-gamma and formation of diacylglycerol (DAG) and inositol triphosphate (IP_3). IP_3 binds to receptors on the endoplasmic reticulum to cause release of intracellular Ca^{2+} stores, which along with DAG, activates protein kinase C (PKC). PKC activates the Raf-MEK-ERK pathway, a signaling cascade that ultimately results in increased transcription of endothelial genes, and consequently, proliferation of endothelial cells. Endothelial cells are the epithelial cells of blood vessels. Other VEGF-A and VEGFR-2 signaling pathways are essential to endothelial cell survival, permeability, and migration (Holmes et al., 2007).

Current anti-angiogenic drugs include tyrosine kinase inhibitors and Fumagillin (Ellis & Hicklin, 2008). TNP-470 is a Fumagillin analog that inhibits VEGF (De Bandt et al., 2000) synthesis by irreversibly binding to and inactivating methionine aminopeptidase-2 (METAP-2), which causes arrest of the G_1 phase of the endothelial cell cycle ("NCI Drug Dictionary", n.d., para. 1). The specific mechanism by which endothelial cell growth interruption occurs is still under study, though it is currently believed that TNP-470 covalently binds to the METAP-2 active site's catalytic ^{231}His and inhibits the early steps of noncanonical Wnt pathway (Hines et al., 2010).

Vascularization has been found to be a critical component of the bone healing process. The use of non-steroidal anti-inflammatory drugs (NSAIDs) in rats have been shown to both delay and restrict the complete healing of femoral bone fractures, particularly by delayed maturation of callus that was observed in the analysis of histology and mechanical testing (Altman et al., 1995). NSAIDs act via inhibition of the

cyclooxygenase pathway to reduce prostaglandin release. Prostaglandins are known to cause vasodilation, and thus increase blood flow, to an area of stress where inflammation occurs. Such evidence supports the claim that vascularization plays a pivotal role in bone repair (Wheeler & Batt, 2005).

Vascularization has also been shown to significantly increase in areas of bone injury. A study of dogs undergoing lengthening of the tibia at the proximal metaphysis showed, by quantitative technetium scintigraphy, a ten-fold increase in blood flow compared to the control at the distraction site. This study not only suggests that blood flow is crucial to bone disturbances but also proposes distraction osteogenesis as a means of improving bone healing by promoting vascularization (Aronson, 1994). In addition, Dr. Tomlinson and his colleagues created adult rat forelimb stress fractures using a mechanical loading process and showed that when Fumagillin was used to block angiogenesis, there was diminished vascularization and woven bone formation. Whether blood in the vascularization of fractured bone carries essential mineralization components or skeletal stem cells, or both, is a topic still under study today (Tomlinson et al., 2012).

The necessity of angiogenesis in bone formation is further supported by findings of a positive correlation between VEGF and up-regulation of BMP2 expression in endothelial cells. When bovine and human endothelial cells were stimulated with recombinant human VEGF, *BMP2* mRNA expression increased by 2 to 3 times after just 24-48 hours post-stimulation. It was thus concluded that VEGF is crucial not only to angiogenesis but also to osteogenesis, suggesting a relationship between the two processes (Bouletreau et al., 2002). As anticipated, another study used VEGF antagonist

SFLT1 to show a notable decrease in BMP2-induced bone formation from muscle-derived stem cells (Peng et al., 2005).

Though angiogenesis has been shown to be critical in both the healing and development of bone, a clearer understanding of when angiogenesis plays a role in endochondral ossification is needed. It is has been known that vascularization brings osteoprogenitors into the cartilage matrix so that mineralization may take place (Mescher, 2010, p. 130). But more recently, there is evidence of angiogenesis playing a key function in mesenchyme condensation during limb development, as it has been shown that the vascular patterning surrounding mesenchymal condensations undergo substantial rearrangement (Eshkar-Oren et al., 2009).

Bone Grafts & Demineralized Bone Matrix

Current methods of bone repair include the implementation of a variety of bone grafts. Osteoconductive materials include allograft bone and calcium sulfates or phosphates, which serve as a scaffold that recruits an ingrowth of osteoblasts and vascularization at the site of implantation (Bauer & Muschler, 2000). On the other hand, osteoinductive grafts function by attracting mesenchymal stem cells to its location, where they differentiate into bone cells to form bone. An example of this is demineralized bone matrix (DBM), a putty-like material that is used in bone repair.

DBM is prepared commercially by harvesting and processing human soft tissue cortical bone into small particles. The bone particles are then demineralized in an agent such as hydrochloric acid and washed to create DBM powder. To finalize the process, the

DBM powder is combined with a denatured collagen solution to produce material of a putty consistency. DBM's bone formation characteristics are attributed to BMP2 activity, which has been found to increase osteoinductive potential and promote osteogenic differentiation of mesenchymal stem cells; however, the exact mechanism by which DBM causes bone growth is still unclear (Pietrzak et al., 2005). DBM is readily available and often used in the clinical setting for periodontal and orthopedic cases (Maddox et al., 2000).

Since BMP2 has been demonstrated to play a necessary role in bone repair, its osteoinductive properties have been proposed for therapeutic uses to generate cartilage and bone (Wozney & Rosen, 1998). A synthetic peptide of BMP2 that was administered in rats using an alginate gel showed that BMP2 was capable of not only inducing ectopic bone formation but also accelerating bone repair in fractures (Saito et al., 2005). Thus, a recombinant human bone morphogenetic protein 2 (rhBMP-2) was produced and further tested through implantation in rat bone defects. This provided further support for the healing potential of BMP2 via induction of local endochondral bone formation (Yasko et al., 1992). Clinical testing showed improved surgical outcome with the use of rhBMP-2, ranging from decreased blood loss to shorter use of operating room time. As a result, rhBMP-2 was FDA-approved for human use in the orthopedic setting, such as for fracture healing (Khan & Lane, 2004). rhBMP2, among other recombinant human BMPs, is often administered using a collagen matrix as a carrier (Sharma et al., 2012). Common examples of collagen matrix vehicles are collagen sponges (Geiger et al., 2003) and DBM (Pietrzak et al., 2006).

Angiogenesis Mechanism in Skeletal Biology

There is clear evidence that a link exists between angiogenesis and bone formation, as shown by studies such as Gerber's discovery of a positive correlation between VEGFR and BMP2 expression in endothelial cells that were stimulated with VEGFR (Bouletreau et al., 2002) and Tomlinson's findings of diminished bone formation in fracture healing post-administration of an anti-angiogenic agent (Tomlinson et al., 2013). In prior studies from our laboratory using a model of distraction osteogenesis to induce new bone formation, endothelial cells and smooth muscle cells in new vessels that formed in the surrounding muscle of the bone regenerate were shown to be the primary source of BMP2 production (Matsubara et al., 2012). Despite the prevalence of claims regarding angiogenesis to be a critical component in the bone formation process, little is known of the exact mechanism by which angiogenesis supports endochondral bone formation and the role it plays in stem cell recruitment and cartilage development . Manipulating angiogenesis using TNP-470 in an *in vivo* model indicative of bone formation, via DBM, allowed us to more closely observe the role of angiogenesis in endochondral ossification. In turn, we identified the requirement for angiogenesis considerably earlier in endochondral ossification. A better understanding of this mechanism will provide additional insight into physiological bone development and improve current therapies for fractures.

SPECIFIC AIMS

We hypothesize that angiogenesis is needed to support endochondral ossification *in vivo*. The main objective of this study is to gain a clearer understanding of the mechanism of angiogenesis in bone development, and in order to do so, we will:

- Develop an *in vivo* model for *de novo* bone formation, which will take form in the implantation of DBM proximal to the femur via survival surgeries in mice.
- Utilize an anti-angiogenic agent, specifically TNP-470, to manipulate vascularization of the bone formation model.
- Conduct the experiment at critical time points of bone formation: day 2 for analysis of the initial stages of bone development, day 8 for investigation during the cartilaginous stages of endochondral ossification, and day 16 for the evaluation of mineralization.
- Examine bone mineralization using x-rays and micro-computed tomography (micro-CT) analysis.
- Uncover the mechanism by which angiogenesis occurs using a multitude of quantitative real-time polymerase chain reaction (qRT-PCR) primers representative of the key steps of endochondral ossification.
- Discuss a possible mechanism for angiogenesis in endochondral ossification.

We hope these studies will shed light on the mechanism by which angiogenesis specifically occurs in endochondral ossification, a topic that is currently unclear and has not been extensively studied in the past.

METHODS

Animals & Surgery

All animal studies were approved by the Institutional Animal Care and Use Committee at Boston University. The mice were housed under standard conditions. Mice of strain B6,129S7-Rag1$^{tm1/MOM}$/J aged 10 to 13 weeks from The Jackson Laboratory were utilized in this study. The mice underwent surgery in which 50 mg of GRAFTON® DBM Putty was implanted bilaterally and proximal to the femur. During the first 36 hours of post-operative care, both experimental and control mice were subcutaneously injected three times with 0.1 mL of Buprenex® as pain medication and once with 0.01 mL of Baytril® as antibiotics. The mice were euthanized at three time points, day 2, 8, and 16 post-surgery. Five experimental animals were enrolled for each time point and subjected to TNP-470 injections. Control animals did not receive injections (n=4-7 per time point). A second set of animals were enrolled to serve as day 0 and did not receive surgery (n=5).

TNP-470, Angiogenesis Inhibitor

TNP-470 was obtained from EMD Chemicals, Inc., and a 10% stock solution was created by dissolving 10 mg of TNP-470 with 100 μL of ethanol. The working solution to be injected into the animals was diluted with phosphate buffered saline (PBS) to 5 mg/mL. The first dose of TNP-470 (25 mg/kg) was injected in each mouse subcutaneously, approximately three hours post-surgery. Each consecutive dose was administered approximately 24 hours after the previous dose until the appropriate

experimental time point was reached. The mice were not injected with TNP-470 on the day of harvest.

Harvest & X-rays

On the day of harvest, the mice were euthanized via carbon dioxide inhalation followed by cervical dislocation. X-rays were then promptly taken of the left and right femur using the Faxitron MX-20 Specimen Radiography System, at a setting of 30 kV for 40 seconds, with Kodak BioMax XAR Scientific Imaging Film.

The DBM implant proximal to the left femur was dissected for mRNA analysis, and the tissues were snap-frozen in liquid nitrogen immediately after harvest and stored at -80°C. The skin from the right thigh was removed, leaving the muscle, DBM implant, and femur intact for Micro-CT analysis followed by histological preparation. For these samples, the tissues were first fixed in 4% paraformaldehyde (PFA) at 4°C for one week and then stored in 1X PBS at 4°C until use for the analysis.

Micro-CT Analysis

Sequential micro-CT analysis was performed on three day 8 control samples, five day 8 experimental samples, five day 16 control samples, and five day 16 experimental samples using the SCANCO Medical μCT 40 Scanner. The scans were taken at a voltage of 70 kVp with a current of 114 μA at medium resolution. The integration time was 200 ms, and a conical tube size of 20.5 mm was used. This analysis provided not only a visualization of the DBM implants surrounding the femur but also allowed for the

quantification of bone volume of the DBM implants. Analysis of animals from the day 2 time point was not carried out because previous studies have shown that mineralization was unable to be detected at this time point (unpublished data).

RNA Extraction

RNA extraction was performed by tissue dissociation and chemical extraction of the DBM implants with the Qiagen Tissue Lyser II®. Each tissue sample was placed in a separate 0.2 mL tube with 0.75 mL Qiazol® Lysis Reagent and snap frozen in liquid nitrogen. A Qiagen stainless steel bead 5 mm in diameter was placed in each tube with the frozen sample and lysed in the Qiagen Tissue Lyser II® for approximately 3 minutes, or until the DBM implant was fully ground and thawed. The pink solution was then transferred to a new 2-mL tube, and 1 mL Qiazol® Lysis Reagent was added to each tube. The samples were then left on ice for at least 2 minutes before adding 0.2 mL chloroform obtained from Sigma-Aldrich®. The samples were vortexed, left on ice for 2 minutes, and then vortexed thoroughly again. They were followed with centrifugation for 15 minutes at 4°C and 14000 rpm.

Approximately 0.75 mL of the resulting aqueous phase of each tube was transferred to a new Eppendorf Tube®, and an equal volume of isopropanol from Sigma-Aldrich® was added. Each tube was inverted several times to turn the liquid from cloudy to clear and centrifuged for 30 minutes at 4°C and 14000 rpm.

The supernatant was removed again, and the pellet was washed with 0.5 mL of 70% ethanol from Sigma-Aldrich®, then centrifuged for 5 minutes at 4°C and 14000

rpm. Ethanol washing of the sample was repeated once more. The ethanol was finally removed, and the tubes were left open for approximately 30 minutes so that each pellet could dry. The dry pellets were then dissolved in 0.03 to 0.1 mL RNase-free water, preferably 0.1 mL depending on the size of the pellet, by pipetting up and down. The resulting extracted RNA was stored at -80°C.

The integrity of the extracted RNA was analyzed using gel imaging and spectrophotometry. One µL of each sample was loaded onto a 1% gel, made with UltraPure™ agarose from Invitrogen and GelStar™ Nucleic Acid Gel Stain from Lonza Group, along with 2 µL of 6X Agarose Gel Loading Dye from Boston BioProducts diluted with 7 µL of RNase-free water. The appearance of bright bands on the gel confirmed the presence of intact RNA. Detection by spectrophotometer of a ratio of absorbance at 260 nm to absorbance at 280 nm in the range of 1.8 to 2.1 is desired to show that the RNA is of acceptable quality.

cDNA Production

RNase-free water was added to 2 µg of the previously extracted RNA to produce a total volume of 10.4 µL in a 0.2-mL PCR tube. The TaqMan® Reverse Transcription Reagents kit from Applied Biosystems® was utilized, and a mixture of the following reagents and enzymes was produced: $MgCl_2$ solution, dNTP Mix, 10X RT Buffer, Random Hexamers, RNase Inhibitor, and TaqMan® Reverse Transcriptase. 19.6 µL of this mixture was added to each sample to bring the total volume of the PCR tube to 30 µL. The samples were then placed in an Eppendorf Mastercycler® Personal thermal

cycler to undergo PCR at the following settings: 25°C for 10 minutes, 37°C for 60 minutes, 95°C for 5 minutes, and finally, a 4°C hold. RNase free water was used to make a 1:25 dilution of the resulting cDNA, which was stored at -20°C.

Primer	Catalog Number
Normalization Primer	
18s	Mm03928990_g1
Angiogenesis Primers	
Vegfa	Mm00437304_m1
Vegfr2 (Kdr)	Mm00440099_m1
α-Sma (Acta2)	Mm00725412_s1
VE-cadherin (Cdh5)	Mm03053719_s1
Pecam1	Mm01242584_m1
Stem Cell Primers	
Sox2	Mm03053810_s1
Nanog	Mm02384862_g1
Prx1 (Prrx1)	Mm00440932_m1
Pax7	Mm01354484_m1
Cartilage Primers	
Sox9	Mm00448840_m1
Sox5	Mm01264584_m1
Sox6	Mm00488393_m1
Col2a1	Mm00491889_m1
Acan	Mm00545794_m1
Col10a1	Mm00487041_m1
Gdf5	Mm00433564_m1
Condensation Primers	
N-cadherin (Cdh2)	Mm01162497_m1
Ncam1	Mm01149710_m1
Bone-Associated Primers	
Bmp2	Mm01340178_m1
Osterix (Sp7)	Mm04209856_m1
Osteocalcin (Bglap1)	Mm03413826_m1
Dmp1	Mm01208363_m1
Trap5b (Acp5)	Mm00475698_m1

Table 1. qRT-PCR Primers. Primers and their respective catalog numbers.

qRT-PCR

qRT-PCR was carried out using 10 µL TaqMan® Universal PCR Master Mix from Applied Biosystems® and 1 µL TaqMan® Gene Expression Assays from Applied Biosystems® for 9 µL of each sample. A list of primers used in this study can be found in Table 1. A 96-well qPCR plate was used, and doublets of each sample were run. RNase-free water was used in lieu of sample for negative controls. The plate was then spun down in a centrifuge, covered with a clear film, and analyzed using an ABI 7700 Sequence Detector® from Applied Biosystems®. The qRT-PCR reaction was set up as follows and repeated for 40 cycles: 50°C for 2 minutes, 95°C for 10 minutes, 95°C for 15 seconds, and 60°C for 1 minute. For analysis of qRT-PCR, Microsoft® Excel® 2011 was used to calculate gene expression of the control and treated DBM implants for each primer. Values were normalized to non-operated B6,129S7-Rag1$^{tm1/MOM}$/J mouse femurs as a control in order to calculate gene expression fold change compared to control femurs.

Statistical Analysis

Statistical analysis of the data was performed using GraphPad Prism® 6 and Microsoft® Excel® 2011. GraphPad Prism® 6 was used to create graphs comparing calculated bone volume from the micro-CT scans of the control and treated DBM implants at time points day 8 and day 16. Statistical significance was calculated using a multiple comparison t-test via the Holm-Sidak method, where significance was $p<0.05$.

RESULTS

X-ray Imaging

Mouse femurs were x-rayed immediately after harvest to identify the DBM implant on each femur. Day 2 control and experimental mice (treated with TNP-470) showed no mineralization of the DBM implant. Day 8 control mice showed a small growth of bone on the femur, while day 8 experimental mice showed no observable growth. By day 16, the control mice showed a greater growth of bone on the femur. However, day 16 experimental mice x-rays showed no mineralization of the DBM implant, similar to day 8 experimental mice (Figure 2).

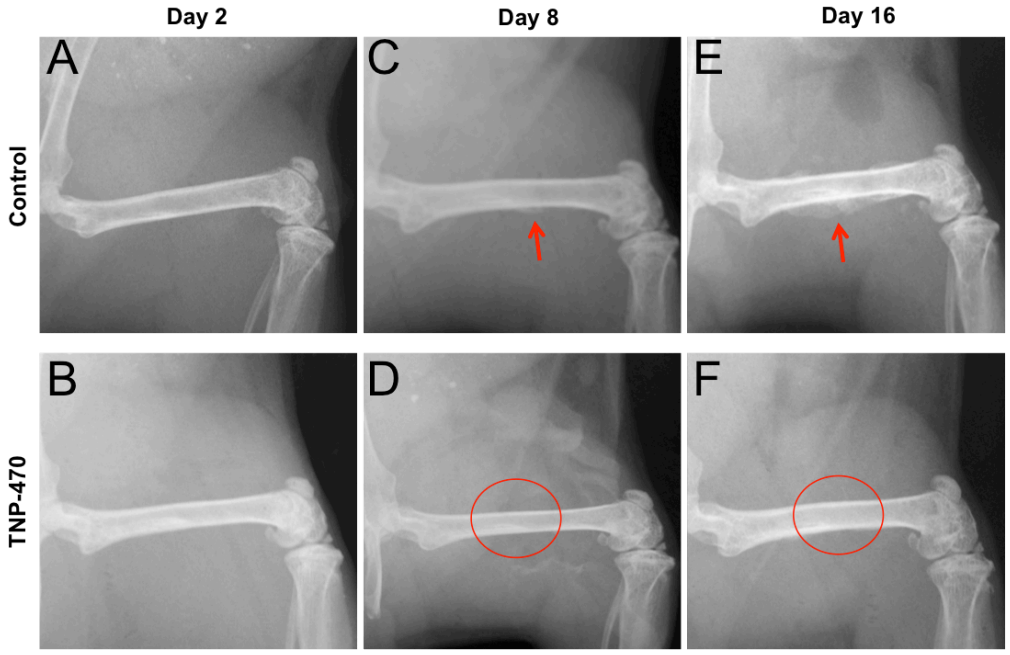

Figure 2. X-ray imaging of DBM implant. DBM was implanted proximal to mouse femurs, and x-rays were taken. (A-E) Arrow indicates site of DBM implantation, while circle indicates site of implant with no resulting growth. (A) Day 2 control DBM implant. (B) Day 2 DBM implant of mouse treated with TNP-470. (C) Day 8 control DBM implant. (D) Day 8 DBM implant of mouse treated with TNP-470. (E) Day 16 control DBM implant. (F) Day 16 DBM implant of mouse treated with TNP-470.

Micro-CT Analysis

Micro-CT analysis was used to both visualize and calculate the bone volume of the DBM implants for the day 8 and day 16 time points. Both time points showed a significant decrease in bone volume development in the animals treated with TNP-470. At the day 8 time point, control animals showed an average bone volume of 0.639 mm^3 (+/- 0.121, n=3), while the experimental mice lacked a measurable amount of bone growth. By day 16, the average bone volume for the controls was 1.839 mm^3 (+/- 0.344, n=5). This was significantly different ($p<0.05$) when compared to the day 16 experimental mice, which had an average bone volume of 0.418 mm^3 (+/- 0.148, n=5) (Figure 3).

Angiogenesis Studies

Angiogenesis was detected within the harvested implant by analyzing the relative expression of five marker genes known to be associated with endothelial cells and blood vessel growth; these were *Vegf-a*, *Vegfr-2*, alpha smooth muscle actin (*α-Sma*), vascular endothelial cadherin (*VE-cadherin*), and platelet endothelial cell adhesion molecule 1 (*Pecam1*) (Figure 4). *Vegf-a* relative gene expression at day 2 for control DBM implants showed a mean fold change of 1.630 (+/- 0.288, n=3). There was a significant increase in expression for the DBM implants of mice treated with TNP-470 with a fold change expression of 25.614 (+/- 6.639, n=5). Similar results were also found in the day 8 samples, which showed *Vegf-a* expression of 1.192 (+/- 0.426, n=7) in the controls and 10.494 (+/- 1.733, n=5) in the TNP-470 treated samples ($p<0.005$). The trend was similar

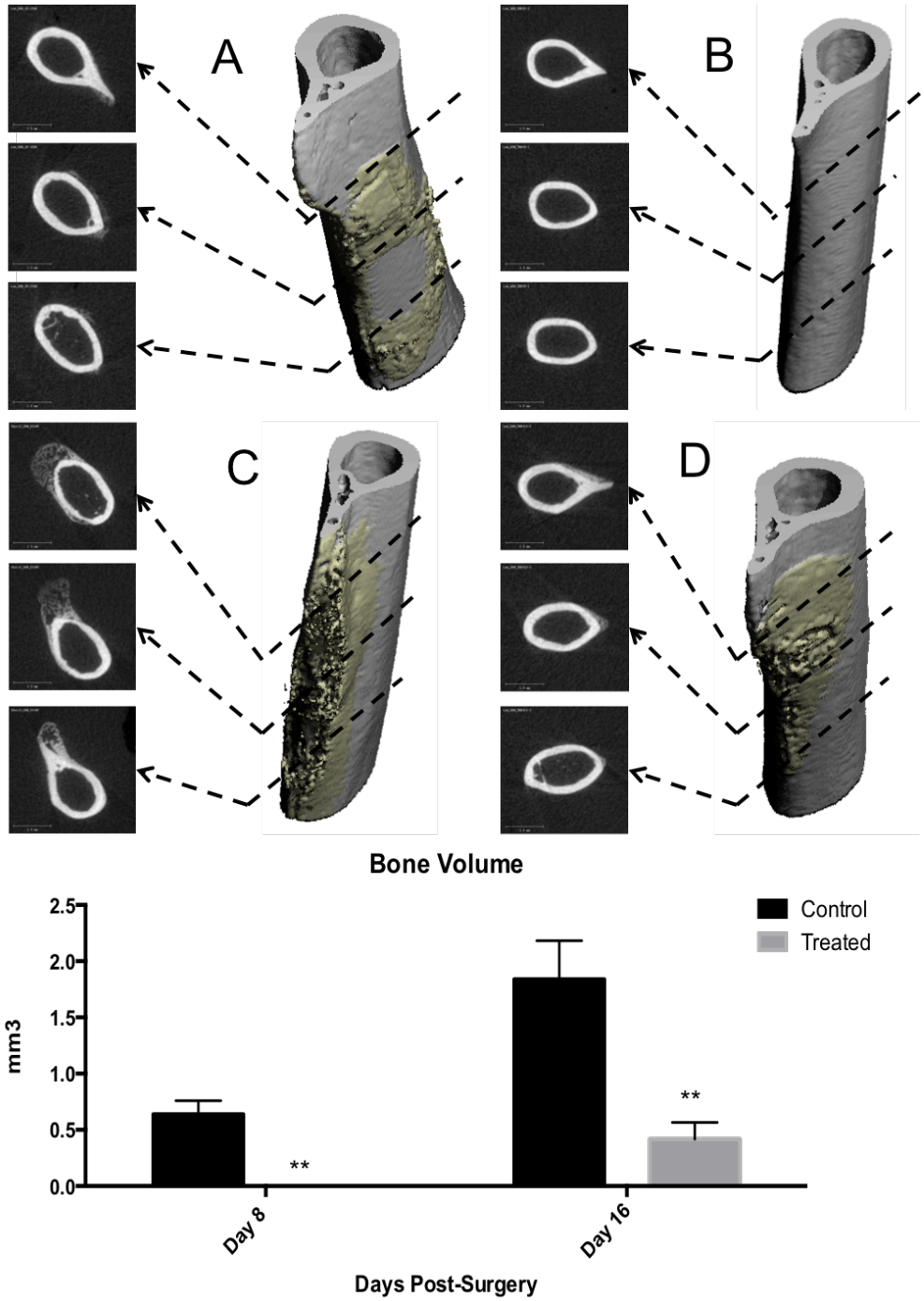

Figure 3. Micro-CT scans of femur and DBM implant. (A-D) Femur is displayed in grey while implant is displayed in yellow. Black arrows point to slices through the sample. Individual bone slices show cross-sectional view of bone in white and surrounding implant in textured grey. (A) Day 8 Control. (B) Day 8 experimental. (C) Day 16 Control. (D) Day 16 Experimental. (E) Bone volume at day 8 and 16 for control and TNP-470-treated samples. * = $p<0.05$, ** = $p<0.005$.

at day 16, though expression was overall decreased. Controls showed a mean fold change of 0.537 (+/- 0.069, n=5), and the treated DBM implants demonstrated a significant increase in fold change of 1.170 (+/- 0.242, n=5), (Figure 4A). The expression of *Vegfr-2* and *α-Sma* were also increased with TNP-470 treatment at all three time points. However, these differences were not significant ($p>0.05$) in *Vegfr-2* (Figure 4B) and only significant at day 8 and day 16 ($p<0.05$) for *α-Sma* (Figure 4C).

Although there was less *VE-cadherin* expression in day 2 control DBM implants at a mean fold change of 5.143 (+/- 1.644, n=3) than day 2 experimental DBM implants at a mean fold change of 99.458 (+/- 43.639, n=5), this difference was not statistically significant ($p>0.05$). However, a significant decrease ($p<0.05$) was observed in *VE-cadherin* expression from 5.949 (+/- 0.675, n=7) in the control samples to 2.882 (+/- 1.105, n=5) in the experimental samples. At day 16, control implants had a mean fold change of 3.239 (+/- 0.733, n=5), and the experimental implants had a mean fold change of 17.175 (+/- 3.346, n=5); this difference was significant ($p<0.005$) (Figure 4D).

A statistically significant decrease in *Pecam1* expression was observed at all three time points ($p<0.05$). Day 2 control samples had a mean fold change of 1.629 (+/- 0.410, n=4), while their corresponding experimental samples had a mean fold change of 0.611 (+/- 0.193, n=5). At day 8, *Pecam1* expression decreased from 1.478 (+/- 0.161, n=7) in the control DBM implants to 0.104 (+/- 0.022, n=5) in the treated DBM implants. Day 16 control samples displayed a mean fold change of 1.476 (+/- 0.250, n=5), while the experimental samples showed a mean fold change of 0.055 (+/- 0.006, n=5) (Figure 4E).

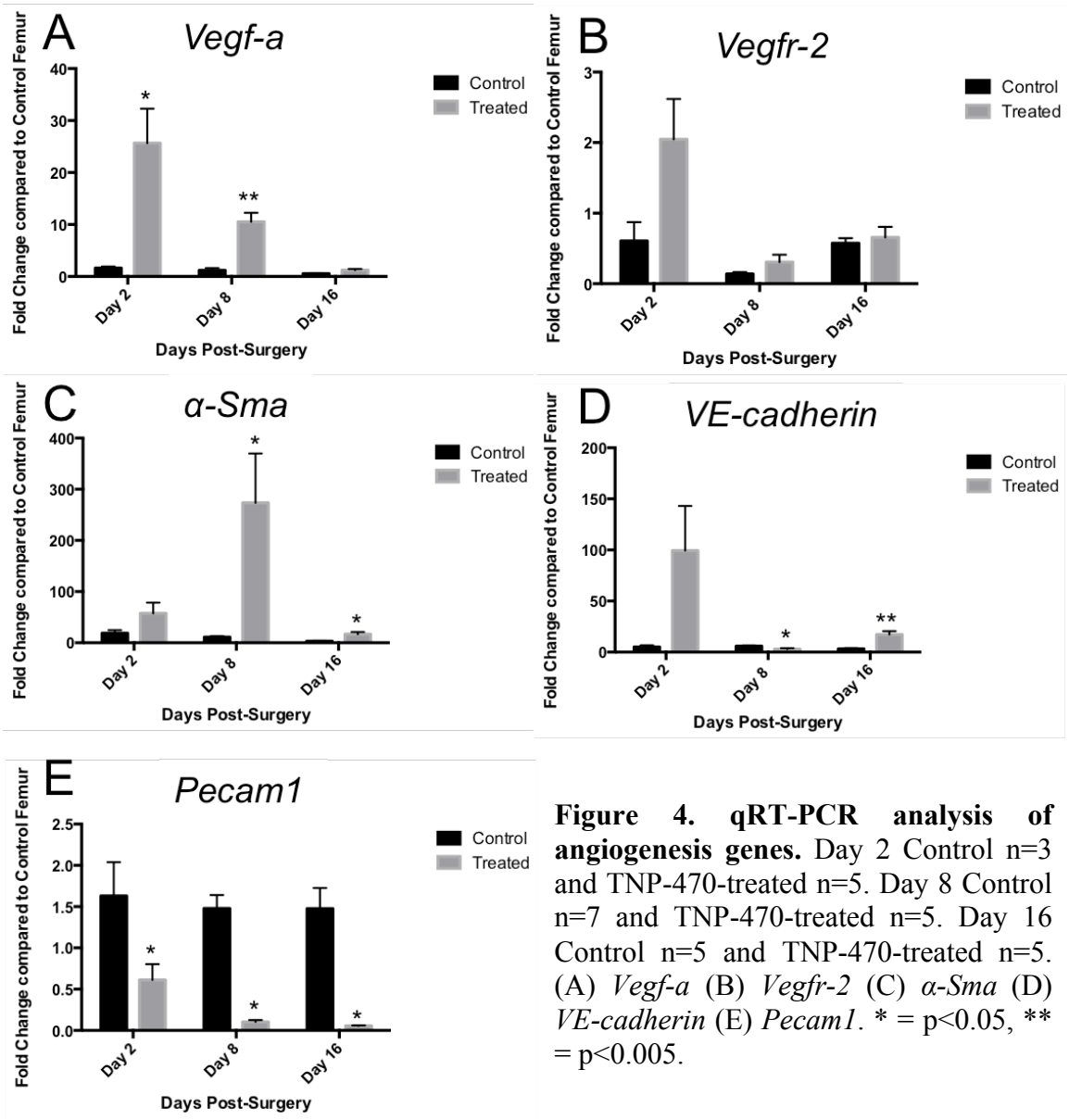

Figure 4. qRT-PCR analysis of angiogenesis genes. Day 2 Control n=3 and TNP-470-treated n=5. Day 8 Control n=7 and TNP-470-treated n=5. Day 16 Control n=5 and TNP-470-treated n=5. (A) *Vegf-a* (B) *Vegfr-2* (C) *α-Sma* (D) *VE-cadherin* (E) *Pecam1*. * = $p<0.05$, ** = $p<0.005$.

Stem Cell Studies

The stem cell markers chosen for this analysis were *Sox2*, *Nanog*, paired related homeobox protein 1 (*Prx1*), and paired box 7 (*Pax7*). Only the day 2 time point was observed for these genes, as day 2 was the earliest time point in our study and is the initial step in endochondral ossification. There was no significant difference in *Sox2* or

Prx1 expression between the control and treated DBM implants ($p>0.05$). *Sox2* control DBM implants showed a mean fold change of 96.879 (+/- 59.778, n=3), while the experimental samples showed a mean fold change of 76.469 (+/- 69.073, n=5) (Figure 5A). As for *Prx1*, the control samples had a mean fold change of 25.604 (+/- 4.361, n=4), and the treated samples had a mean fold change of 14.585 (+/- 6.520, n=5) (Figure 5B).

In contrast, substantial decreases in *Nanog* and *Pax7* expression were observed in the DBM implants of TNP-470-treated mice. Though the difference in *Nanog* expression was insignificant ($p=0.08$), there was still a robust difference between a mean fold change of 81.194 (+/- 50.568, n=3) in the control samples and a mean fold change of 3.321 (+/- 1.758, n=5) in the experimental samples (Figure 5C). There was a significant difference in *Pax7* expression ($p<0.005$), with a control DBM implant mean fold change of 863.748 (+/- 213.764, n=4) decreasing to a treated DBM implant mean fold change of 18.870 (+/- 16.417, n=5) (Figure 5D).

Cartilage Studies

The expression of these stem cell genes led us to analyze the earliest markers of chondrogenesis: *Sox9*, *Sox5*, and *Sox6*. There was expression of *Sox9* at day 2 and day 8 but minimal expression at day 16. There was no significant difference of *Sox9* expression between the control and experimental samples ($p>0.05$). Day 2 control samples had a mean fold change of 0.578 (+/- 0.251, n=3), and the corresponding experimental samples had a mean fold change of 1.486 (+/- 0.516, n=5). Day 8 samples showed an overall increase in *Sox9* expression, with a mean fold change of 9.435 (+/- 2.693, n=5) for the

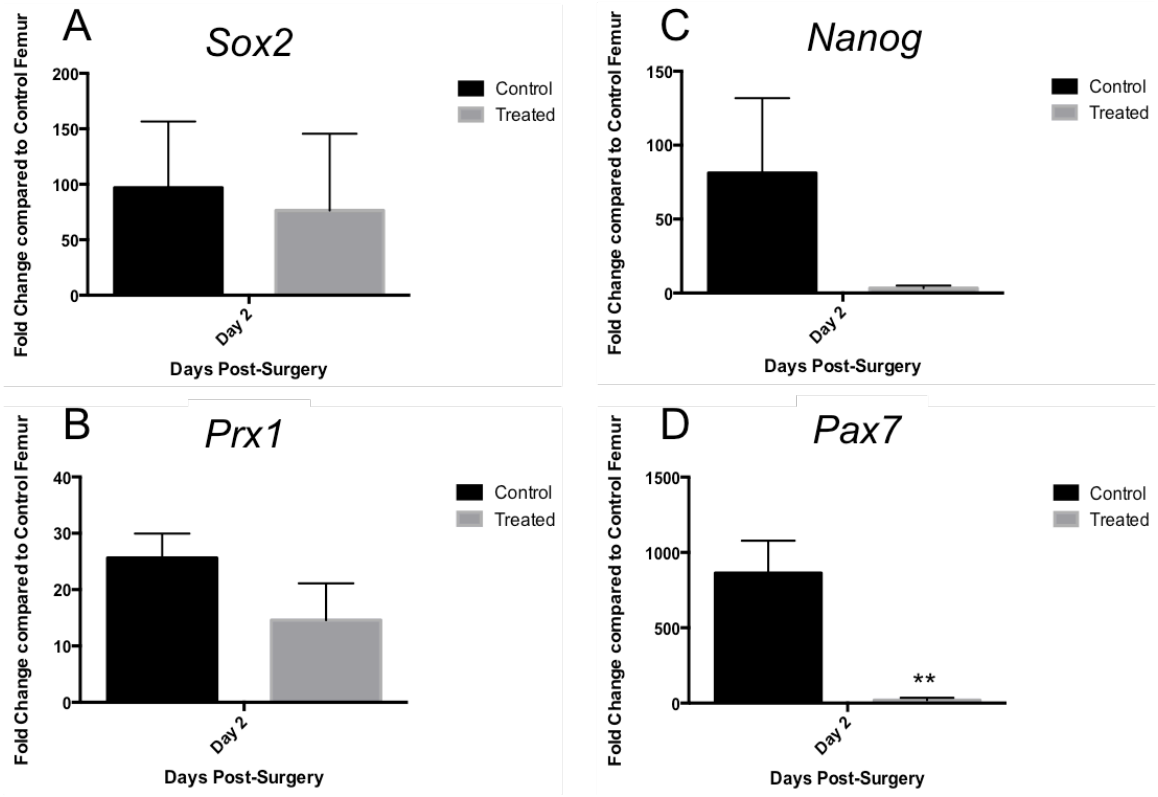

Figure 5. qRT-PCR analysis of stem cell markers. Day 2 control n=3 and TNP-470-treated n=5. (A) *Sox2* (B) *Prx1* (C) *Nanog* (D) *Pax7* * = $p<0.05$, ** = $p<0.005$.

control DBM implants and a mean fold change of 7.237 (+/- 2.289, n=5) for the treated DBM implants (Figure 8A). Day 16 control samples had a mean fold change of 0.693 (+/- 0.163, n=5), while the experimental DBM implants had a mean fold change of 4.496 (+/- 0.801, n=5). This difference was statistically significant ($p<0.005$) (Figure 6A).

Sox5 and *Sox6* showed decreased expression in the experimental samples at all three time points. This difference in *Sox5* expression was significant at all three time points ($p<0.05$). Day 2 control samples showed a mean fold change of 2.197 (+/- 0.339, n=4), which significantly decreased ($p<0.05$) to 0.947 (+/- 0.372, n=5) in the corresponding experimental samples. Day 8 control samples showed an expression of 8.888 (+/- 1.297, n=7), and there was less expression in the day 8 experimental samples

at 1.092 (+/- 0.206, n=5); this difference was statistically significant ($p<0.005$). Day 16 control samples had a mean fold change of 4.247 (+/- 1.219, n=5), and day 16 treated samples had a decreased mean fold change of 1.032 (+/- 0.064, n=5); this change was also significant ($p<0.05$) (Figure 6B). The decrease in *Sox6* expression between the control and TNP-470 treated samples was only significant at day 8 and day 16 ($p<0.005$) (Figure 6C). There was overall less *Sox6* expression compared to *Sox5* expression in all samples.

Additional genes in the early progression of chondrogenesis include the condensation genes *N-cadherin* and *Ncam1*. *N-cadherin* showed decreased expression at all three time points, though the decrease at day 2 was not statistically significant ($p>0.05$). Day 2 control samples showed a mean fold change of 0.178 (+/- 0.027, n=4), while the corresponding experimental samples showed a mean fold change of 0.105 (+/- 0.056, n=5). Day 8 control samples had an expression of 0.593 (+/- 0.054, n=7), and the experimental samples showed a decreased expression of 0.104 (+/- 0.022, n=5). At day 16, control DBM implants with a *N-cadherin* expression of 0.585 (+/- 0.073, n=5) decreased to an expression of 0.055 (+/- 0.006, n=5) in the treated DBM implants (Figure 7A). *Ncam1* showed similar results, with decreased expression at all three time points that were statistically significant at day 8 ($p<0.005$) and day 16 ($p<0.05$) (Figure 7B). There was overall greater expression of *Ncam1* in all samples compared to *N-cadherin*. The marker genes of *Col2a1*, *Acan*, *Col10a1*, and growth differentiation factor 5 (*Gdf5*) were chosen for observation of the progression of chondrogenesis and for the detection of cartilage. *Col2a1*, *Acan*, and *Col10a1* were minimally, if not at all, expressed in the day 2

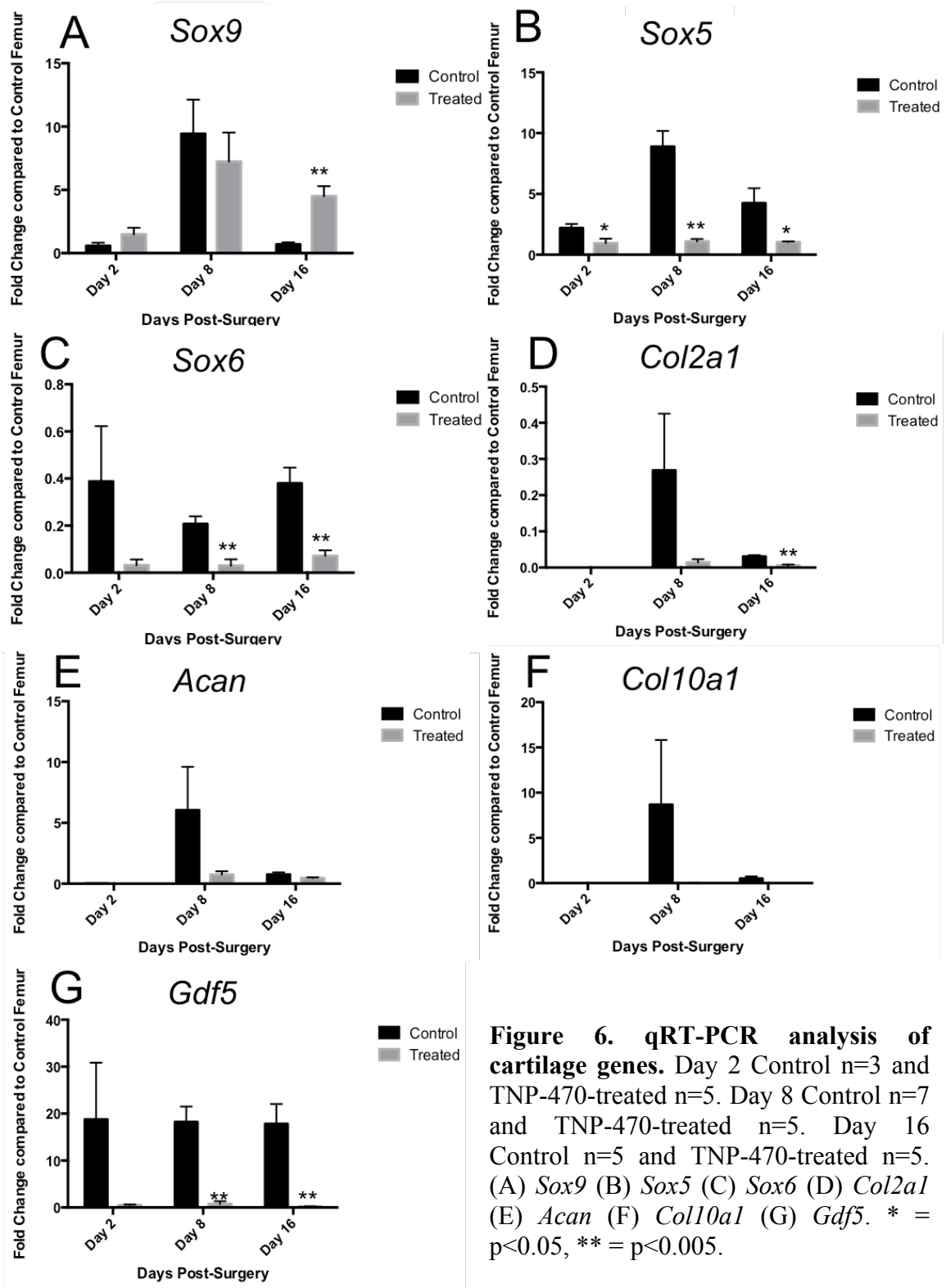

Figure 6. qRT-PCR analysis of cartilage genes. Day 2 Control n=3 and TNP-470-treated n=5. Day 8 Control n=7 and TNP-470-treated n=5. Day 16 Control n=5 and TNP-470-treated n=5. (A) *Sox9* (B) *Sox5* (C) *Sox6* (D) *Col2a1* (E) *Acan* (F) *Col10a1* (G) *Gdf5*. * = $p<0.05$, ** = $p<0.005$.

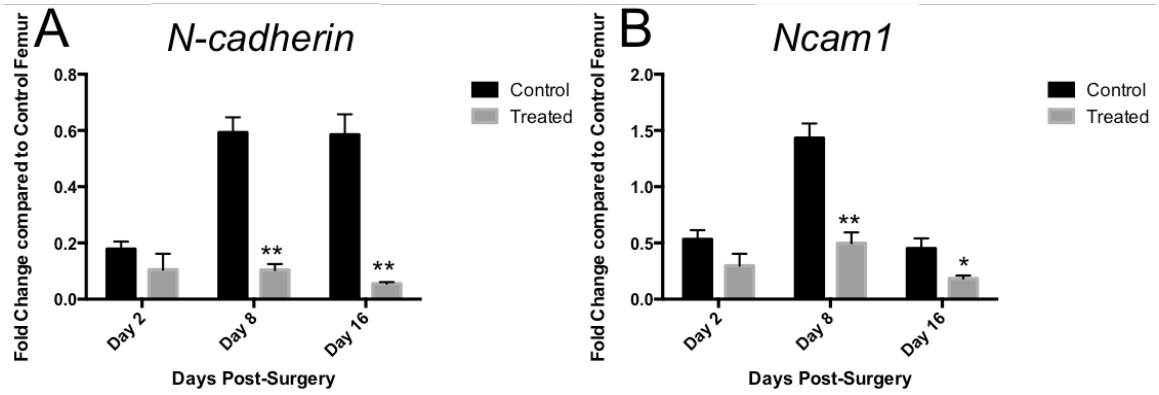

Figure 7. qRT-PCR analysis of condensation genes. Day 2 Control n=3 and TNP-470-treated n=5. Day 8 Control n=7 and TNP-470-treated n=5. Day 16 Control n=5 and TNP-470-treated n=5. (A*) N-cadherin* (B) *Ncam1*. * = $p<0.05$, ** = $p<0.005$, else $p>0.05$

control and TNP-470 treated samples. DBM implants of mice treated with TNP-470 showed a decrease in expression of these three genes for the day 8 and day 16 time points. For *Col2a1*, day 8 control DBM implants showed a relative gene expression of 0.269 (+/- 0.157, n=5), while the corresponding day 8 experimental DBM implants showed a relative gene expression of 0.014 (+/- 0.009, n=5); this difference was found to be insignificant ($p>0.05$). Day 16 control DBM implants showed a mean fold change of 0.031 (+/- 0.004, n=5), and the treated DBM implants showed a mean fold change of 0.006 (+/- 0.003, n=5); this difference was significant ($p<0.005$) (Figure 6D). *Acan* and *Col10a1* showed similar expression trends to *Col2a1*, though the decreases in expression of these genes were found to be only statistically significant at day 2 (Figure 6E & Figure 6F).

Gdf5 showed slightly different results than the other cartilage markers because there was expression in the day 2 control samples. However, it still showed decreased gene expression at all time points. Though results of the day 2 time point were not

statistically significant ($p>0.05$), there was still an observed decrease of expression from 18.743 (+/- 12.107, n=4) in the control implants to 0.488 (+/- 0.156, n=5) in the experimental implants. At day 8, the control samples had a mean fold change of 18.220 (+/- 3.297, n=7) that decreased to 0.734 (+/- 0.619, n=5) in the treated samples. As for day 16, the control DBM implants showed a mean fold change of 17.818 (+/- 4.245, n=5), while the experimental DBM implants showed less *Gdf5* expression at a mean fold change of 0.207 (+/- 0.046, n=5). These decreases were statistically significant ($p<0.005$) (Figure 6G).

Bone Studies

qRT-PCR analysis of genes involved in bone formation and remodeling showed a decrease in expression in implants following treatment of TNP-470. The following primers were chosen for the purpose of this evaluation: *Bmp2*, *Osterix*, *Osteocalcin*, *Dmp1*, and *Trap5b*.

Bmp2 showed decreases in expression at all three time points. At day 2, there was a mean fold change of 1.889 (+/- 0.695, n=4) in the control samples that decreased to a mean fold change of 1.524 (+/- 0.717, n=5) in the TNP-470 treated samples, but this was not significant ($p>0.05$). Day 8 control samples showed a relative gene expression of 1.100 (+/- 0.116, n=7), while the corresponding experimental samples showed decreased gene expression to 0.165 (+/- 0.057, n=5, $p<0.005$). Day 16 control samples had a mean fold change of 1.33 (+/- 0.179, n=5), while day 16 TNP-470 treated samples had a smaller mean fold change of 0.304 (+/- 0.059, n=5, $p<0.005$) (Figure 8A).

Osterix, *Osteocalcin*, and *Dmp1* showed similar results in gene expression. All three of these markers for bone mineralization showed minimal to no expression at day 2 and decreased expression in the treated implants at day 8 and day 16. For Osterix, day 8 control DBM implants showed a mean fold change of 1.198 (+/- 0.753, n=5), and the treated DBM implants showed a mean fold change of 0.050 (+/- 0.019, n=5); this difference was not significant ($p>0.05$). A mean fold change of 1.116 (+/- 0.171, n=5) was found for day 16 control DBM implants, whereas a mean fold change of 0.016 (+/- 0.006, n=5) was found for the corresponding DBM implants treated with TNP-470. This decrease in expression was found to be significant ($p<0.005$) (Figure 8B). Results of *Osteocalcin* were similar to those of *Osterix* in that there was a decrease in expression in the TNP-470 treated DBM implants at day 8 and day 16, with statistical significance at day 16 ($p<0.005$) (Figure 8C). As for *Dmp1*, the mean fold change at day 2 in the control DBM implants was 0.0014 (+/- 0.0003, n=3); there was no *Dmp1* expression detected in the day 2 treated samples (n=5), and this decrease in expression was significant ($p<0.005$). Like *Osterix* and *Osteocalcin*, day 8 and day 16 samples showed decreased *Dmp1* expression in the TNP-470 treated DBM implants, with statistical significance at day 16 ($p<0.05$) (Figure 8D).

qRT-PCR analysis of *Trap5b* expression for the detection of bone resorption showed a significant increase ($p<0.05$) at day 2: the control DBM implants showed a mean fold change of 0.176 (+/- 0.030, n=4), and the experimental DBM implants showed a mean fold change of 0.377 (+/- 0.064, n=5). Day 8 samples showed a significant decrease ($p<0.005$) in expression, with control DBM implants displaying a mean fold

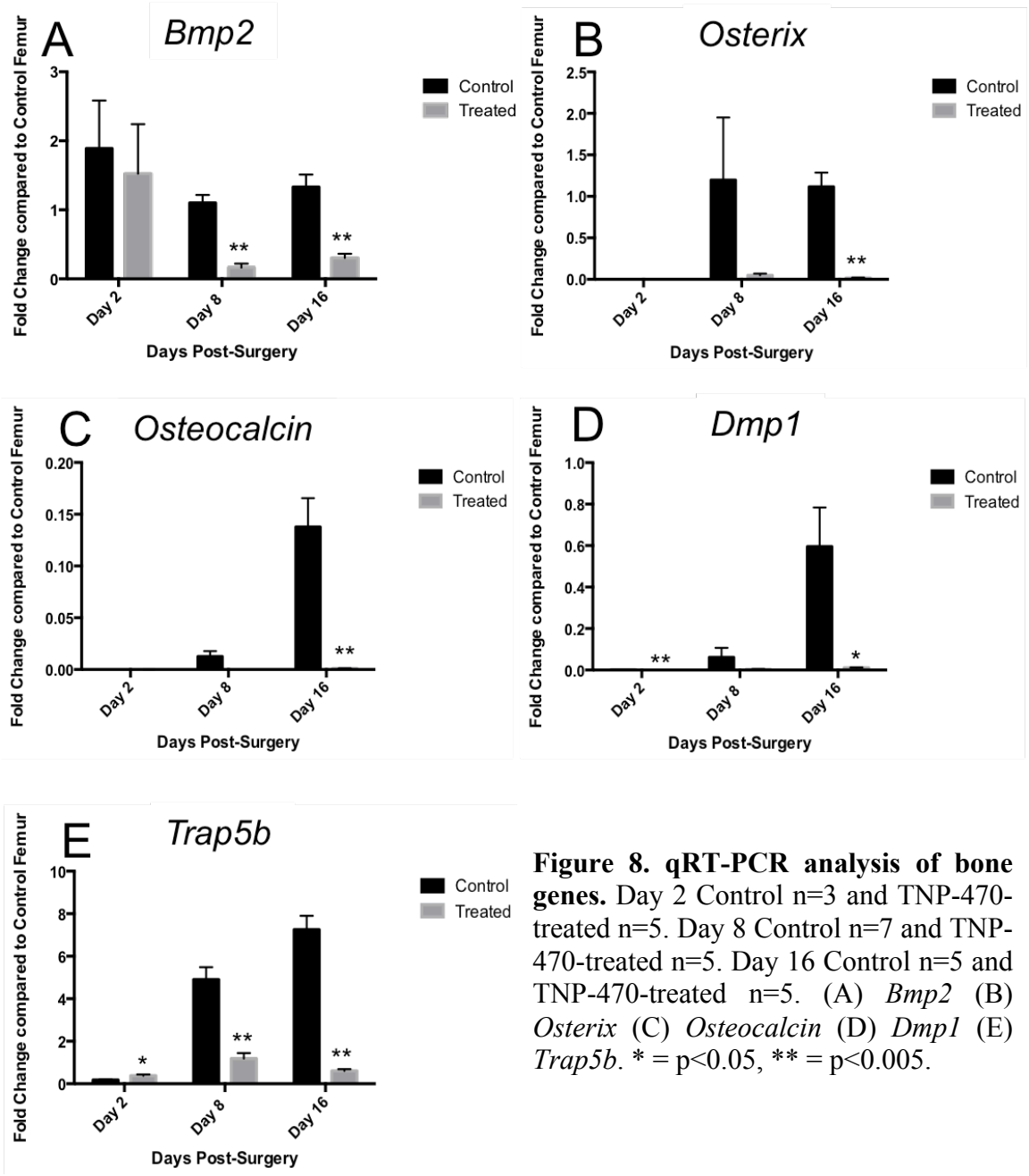

Figure 8. qRT-PCR analysis of bone genes. Day 2 Control n=3 and TNP-470-treated n=5. Day 8 Control n=7 and TNP-470-treated n=5. Day 16 Control n=5 and TNP-470-treated n=5. (A) *Bmp2* (B) *Osterix* (C) *Osteocalcin* (D) *Dmp1* (E) *Trap5b*. * = $p<0.05$, ** = $p<0.005$.

change of 4.907 (+/- 0.579, n=7) and treated DBM implants displaying a mean fold change of 1.184 (+/- 0.264, n=5). The samples showed a significant decrease ($p<0.005$) in *Trap5b* expression at day 16 as well: control DBM implants had a mean fold change of

7.250 (+/- 0.650, n=5) and experimental DBM implants had a mean fold change of 0.605 (+/- 0.083, n=5) (Figure 8E).

DISCUSSION

DBM Implantation as a Model of Bone Formation

The control DBM implantation induced ectopic bone formation at the femur, shown by x-rays as early as day 8 and continued through day 16. We used qRT-PCR data to track endochondral ossification in the control DBM implants. Cartilage markers *Col2a1*, *Acan*, and *Col10a1*, and *Gdf5*, which is responsible for the maintenance of cartilage development (Schwaerzer et al., 2012) are readily expressed at day 8. Day 16 control DBM implants showed presence of the bone markers *Bmp2*, *Osterix*, *Osteocalcin*, *Dmp1*, and *Trap5b*. qRT-PCR data allowed us to reliably track chondrogenesis and mineralization of bone in the DBM control samples.

Micro-CT analysis of this provides not only a three-dimensional rendering of the implant with relation to the femur but also confirms that the mineralization phase of endochondral ossification occurred. There was an increase in bone volume between the day 8 and day 16 time points, which is consistent with the process of endochondral ossification, since day 8 is a time point at which the chondrogenic stage tends to occur and day 16 is a time point at which mineralization is well under way (unpublished data).

Evidence of Angiogenesis Inhibition

The inhibition of angiogenesis was evaluated using qRT-PCR analysis of *Vegf-a*, *Vegfr-2*, *α-Sma*, *VE-cadherin*, and *Pecam1*. As mentioned earlier, VEGF-A and VEGFR-2 play integral roles as ligand and receptor, respectfully, in the tyrosine kinase pathway of

endothelial cell formation (Holmes et al., 2007) and are thus early markers of endothelial cell growth. Although *Vegfr-2* showed increased expression at all three time points, the findings were not statistically significant. There was a significant increase in *Vegf-a* at day 2 and day 8 in the treated sample. In control mice, a small increase in *Vegf-a* expression would recruit vessel formation as a means to support bone formation in the DBM implant. Increased expression in the control implants is also consistent with the finding that vessel formation is induced prior to the onset of chondrogenesis in heterotopic ossification driven by BMP2 (Dilling et al., 2010), since DBM utilizes the properties of BMP2 in *de novo* bone formation. However, in the TNP-470 injected mice, VEGF-A ligand secretion could plausibly increase to compensate for the lack of endothelial cell proliferation and resulting vessel formation; this reasoning is compatible with TNP-470's mechanism of action as an angiogenesis inhibitor, which acts by suspending the endothelial cell cycle, thus preventing cell proliferation and differentiation ("NCI Drug Dictionary", n.d., para. 1).

α-Sma is a marker of myofibroblasts, whose differentiation leads to the synthesis of smooth muscle that makes up blood vessels (Abdalla et al., 2013). *α-Sma* expression was also greater in the TNP-470-treated samples at all three time points, with the change being significant at the day 8 and day 16 time points. The *α-Sma* expression mirrors the *Vegf-a* data in that the lack of vessel formation due to cell cycle arrest causes an increase in ligand, receptor, and vessel components as a compensatory mechanism.

VE-cadherin and *Pecam1* are later markers of endothelial formation. The *VE-cadherin* gene regulates endothelial permeability and is expressed by endothelial cells

(Zeng et al., 2012), while *Pecam1* is a marker for endothelial cell adhesion (Kellermair et al., 2013). *VE-cadherin* only showed a significant decrease in expression at day 8. Although greater expression of *VE-cadherin* occurred in the experimental sample compared to its corresponding control at the day 16 time point, it is possible this is an effect of the anti-angiogenic agent. Previous studies have found that up-regulation of *VE-cadherin* is required to prevent the disassociation of nascent blood vessels (Crosby et al., 2005); thus, it is possible that the increased *VE-cadherin* was a product of the physiological attempt to increase vascularization to the DBM implant in the presence of an angiogenesis inhibitor.

Only *Pecam1* showed significant decrease in expression in the experimental animals at all three time points. PECAM1 is found in the intercellular junctions between endothelial cells, and its lack of expression would correlate with leaky or incomplete vessel formation. Thus, despite the inconsistent results with other angiogenic markers, this may substantiate TNP-470's role in preventing angiogenesis in our mice. However, we are currently performing perfusion studies to verify these claims with increased rigor using micro-CT imaging of vessel formation.

TNP-470 Hinders Bone Mineralization

The x-ray images of the DBM implants post-treatment showed a lack of ectopic bone mineralization compared to the non-treated DBM implants through time. However, the difference appeared to be most robust at day 16. This was supported by the micro-CT images and quantified bone volumes of the ectopic bone.

A closer look at the qRT-PCR data supports these x-ray and micro-CT findings. Expression of *Bmp2*, which promotes osteoblast differentiation (Pietrzak et al., 2005), was significantly decreased at day 8 and day 16. Since *Osterix* (Lee et al., 2003) and *Osteocalcin* (Ducy & Karsenty, 1995) are markers for osteoblasts, *Trap5b* is an osteoclast marker (Henriksen et al., 2007), and *Dmp1* is a gene that is expressed by osteocytes (Kashima et al., 2013), together, the presence of these genes would implicate the occurrence of mineralization and bone turnover. By day 16, a conservative time point for the mineralization of the DBM implant undergoing endochondral ossification and for the completion of chondrogenesis (unpublished data), all four genes display significantly less expression in the DBM implants of mice treated with TNP-470, if any. Thus, bone mineralization is vastly inhibited by the blockage of angiogenesis.

Diminished Chondrogenesis Follows Inhibition of Angiogenesis

The observed decrease in relative gene expression for the early- to late-cartilage markers (*Col2a1*, *Acan*, and *Col10a1*) to almost zero in the TNP-470-treated samples supports the claim that chondrogenesis did not progress. Unexpectedly, analysis of an earlier stage in endochondral ossification yielded similar results. *N-cadherin* and *Ncam1*, which are considered early markers of condensation, showed significant decrease in expression in the mice treated with the anti-angiogenic agent. Since the differences in mean fold change were not as substantial as those of the chondrogenesis markers, such results encouraged further analysis of the earliest stages of chondrogenesis and of pluripotent stem cells.

Angiogenesis is Crucial to the Earliest Endochondral Ossification Stages

Once we learned that mineralization, condensation, and chondrogenesis are all hindered by the inhibition of angiogenesis, we delved deeper into chondrogenesis. Our goal was to isolate the critical point where blood vessels, and the components they provide, are necessary. We analyzed markers of mesenchymal stem cells such as *Sox2*, *Nanog*, *Prx1*, and *Pax7* in day 2 control and treated samples. *Sox2* and *Nanog* are transcription factors involved in the pluripotency of embryonic stem cells (Takahashi & Yamanaka, 2006) that have been shown, in some instances, to work together to mediate embryonic stem cell self-renewal (Gagliardi et al., 2013). *Prx1* works with *Sox2* to maintain adult neural stem cells (Shimozaki et al., 2013) and plays an important role in limb development (Higuchi et al., 2013). Muscle satellite cells express *Pax7*, which is believed to be a requirement for regenerative myogenesis (Maltzahn et al., 2013).

The presence of mesenchymal stem cells was confirmed in all control DBM implants, and *Sox2* and *Prx1* remained in the experimental DBM implants despite treatment with TNP-470. Though there appeared to be considerably less *Nanog* expression in the treated samples, this difference was not statistically significant. *Nanog* has been linked to *Vegfr-2* transcription and thus angiogenesis (Kohler et al., 2010), so it is conceivable that TNP-470 perhaps had an indirect inhibitory effect on *Nanog*. The decreased *Pax7* expression may be explained as an effect of TNP-470 as well, since muscle is believed to play a supportive role in providing vascularization to sites of new bone formation (Liu et al., 2010); therefore, the inhibition of angiogenesis may eliminate the need for muscle formation and, surely, muscle satellite cells. Since TNP-470 did not

affect *Sox2* and *Prx1*, it is probable that the lack of bone formation is not due to the inability to recruit mesenchymal stem cells in the earliest stage of cartilage formation.

Previous studies have shown that BMP signaling, which is utilized by DBM for bone formation (Pietrzak et al., 2005), and the Sox genes work together to promote cartilage differentiation of the limbs (Chimal-Monroy et al., 2003). Analysis of these earliest markers of endochondral ossification yielded interesting results. There was no significant difference in *Sox9* expression between the control and experimental samples at the first two time points and a significant increase in *Sox9* expression at the day 16 time point. The *Sox9* day 2 and day 8 results were expected because *Sox9* is needed for stem cells to commit to differentiation into chondrocytes and is often inactivated after condensation. However, there is increased *Sox9* expression in the treated animals at day 16, when the chondrogenic phase of endochondral ossification is expected to be complete. Increased *Sox9* expression in the day 16 experimental animals but a significant decrease in later cartilage genes suggests that there is commitment to chondrogenesis by this time point but no completion of chondrogenesis with TNP-470 treatment.

Sox9 is also required for activation of the subsequent *Sox5* and *Sox6* transcription factors in chondrogenesis (Akiyama et al., 2002). TNP-470 treatment affected *Sox5* and *Sox6* expression, with decreases in mean fold change at all three time points in both genes. Therefore, less expression of *Sox5* and *Sox6* in the samples treated with anti-angiogenic agent suggests that angiogenesis plays a role in endochondral ossification in the earliest stages of chondrogenesis, even before condensation.

Conclusions & Future Directions

The above results suggest that the DBM implantation is a successful model for *de novo* bone formation and that angiogenesis is needed for chondrogenesis, specifically in the condensation and progression of endochondral bone formation.

This study is fundamental to determining the function of angiogenesis in early endochondral ossification. It is currently accepted that vascularization is needed in the later chondrogenic stage of endochondral ossification and for the mineralization of bone, but its exact role in early the periods of chondrogenic differentiation remains unknown. Our investigation showed that angiogenesis is necessary for cartilage formation and maintenance, which is supported by existing evidence of the necessity of VEGF-A for chondrocyte survival during bone development (Zelzer et al., 2003). Beyond this, our findings also reveal reasonable justification for angiogenesis to occur in the earliest stages of endochondral bone formation, namely during the period after stem cell recruitment of the chondrogenic linage based on *Sox9* expression but preceding further progression based on lack of *Sox5* and *Sox6* activity. This novel claim opposes more recent theories that place VEGF expression and regulation, and thus angiogenesis, in condensed mesenchyme as the initial step in vascularization of limb development (Eshkar-Oren et al., 2009). Successful further experimentation utilizing micro-CT analysis to confirm inhibition of angiogenesis and modeling the process *in vitro* to perform gene silencing will further validate our findings.

A better understanding of the mechanism by which endochondral ossification occurs allows us to improve treatments of skeletal impairments. Specific advances in

research concerning cartilage development progresses the field of cartilage regeneration and cartilage replacement therapy.

REFERENCES

Aarden, E., Nijweide, P., & Burger, E. (1994). Function of osteocytes in bone. *Journal of Cellular Biochemistry*, 55(3), 287-299.

Abdalla, M., Goc, A., Segar, L., & Somanath, P. (2013). Akt1 mediates α-Smooth Muscle Actin Expression and Myofibroblast Differentiation via Myocardin and Serum Response Factor. *The Journal of Biological Chemistry*, 288(46), 33483-33493.

Akiyama, H., Chaboissier, M., Martin, J., Schedl, A., & de Crombrugghe, B. (2002). The transcription factor Sox9 has essential roles in successive steps of the chondrocyte differentiation pathway and is required for expression of Sox5 and Sox6. *Genes & Development*, 16: 2813-2828.

Akiyama, N & Lefebvre, V. (2011). Unraveling the transcriptional regulatory machinery in chondrogenesis. *Journal of Bone & Mineral Metabolism*, 29, 390-395.

Altman, R., Latta, L., Keer, R., Renfree, K., Hornicek, F., & Banovac, K. (1995). Effect of nonsteroidal antiinflammatory drugs on fracture healing: a laboratory study in rats. *Journal of Orthopaedic Trauma*, 9(5), 392-400.

Aronson, J. (1994). Temporal and spatial increases in blood flow during distraction osteogenesis. *Clinical Orthopaedics & Related Research*, 301, 124-131.

Bauer, T. & Muschler, G. (2000). Bone graft materials. An overview of the basic science. *Clinical Orthopaedics & Related Research*, 371, 10-27.

Bouletreau, P., Warren, S., Spector, J., Peled, Z., Gerrets, R., Greenwald, J., & Longaker, M. (2002). Hypoxia and VEGF Up-Regulate BMP-2 mRNA and Protein Expression in Microvascular Endothelial Cells: Implications for Fracture Healing. *Plastic & Reconstructive Surgery*, 109(7), 2384.

Chen, D., Zhao, M., & Mundy, G. (2004). Bone Morphogenetic Proteins. *Growth Factors*, 22(4), 233-241.

Chimal-Monroy, J., Rodriguez-Leon, J., Montero, J., Ganan, Y., Macias, D., Merino, R., & Hurle, J. (2003). Analysis of the molecular cascade responsible for mesodermal limb chondrogenesis: sox genes and BMP signaling. *Developmental Biology*, 257(2): 292-301.

Crosby, C., Fleming, P., Argraves, W., Corada, M., Zanetta, L., Dejana, E., & Drake, C. (2005). VE-Cadherin is not required for the formation of nascent blood vessels but acts to prevent their disassembly. *Blood*, 105(7), 2771-2776.

De Bandt, M., Grossin, M., Weber, A., Chopin, M., Elbim, C., Pla, M., Gougerot-Pocidalo, M., & Gaudry, M. (2000). Suppression of arthritis and protection from bone destruction by treatment with TNP-470/AGM-1470 in a transgenic mouse model of rheumatoid arthritis. *Arthritis & Rheumatism*, 43(9), 2056-2063.

Devlin, R., Du, Z., Pereira, R., Kimble, R., Economides, A., Jorgetti, V., & Canalis, E. (2003). Skeletal Overexpression of Noggin Results in Osteopenia and Reduced Bone Formation. *Endocrinology*, 144(5), 1972-1978.

Dilling, C., Wada, A., Lazard, Z., Salisbury, E., Gannon, F., Vadakkan, T., Gao, L., Hirschi, K., Dickinson, M., Davis, A., & Olmsted-Davis, E. (2010). Vessel formation is induced prior to the appearance of cartilage in BMP-3-mediated hetertropic ossification. *Journal of Bone & Mineral Research*, 25(5), 1147-1156.

Ducy, P. & Karsenty, G. (1995). Two Distinct Osteoblast-Specific cis-Acting Elements Control Expression of a Mouse Osteocalcin Gene. *Molecular & Cellular Biology*, 15(4), 1858-1869.

Ellis, L. & Hicklin, D. (2008). VEGF-targeted therapy: mechanisms of anti-tumour activity. *Nature Reviews Cancer*, 8(8), 579-591.

Eshkar-Oren, I., Viukov, S., Salameh, S., Krief, S., Oh, C., Akiyama, H., Gerber, H., Ferrara, N., & Zelzer, E. (2009). The forming limb skeleton serves as a signaling center for limb vasculature patterning via regulation of Vegf. *Development*, 136, 1263-1272.

Fujikawa, Y., Quinn, J., Sabokbar, A., McGee, J., & Athanasou, N. (1996). The human osteoclast precursor circulates in the monocyte fraction. *Endocrinology*, 137(9), 4061-4064.

Gagliardi, A., Mullin, N., Ying Tan, Z., Colby, D., Kousa, A., Halbritter, F., Weiss, J., Felker, A., Bezstarosti, K., Favaro, R., Demmers, J., Nicolis, S., Tomlinson, S., Poot, R., & Chambers, I. (2013). A direct physical interaction between Nanog and Sox2 regulates embryonic stem cell self-renewal. *The European Molecular Biology Organization Journal*, 32(16), 2231-2247.

Geiger, M., Li R., & Friess, W. (2003). Collagen sponges for bone regeneration with rhBMP-2. *Advanced Drug Delivery Reviews*, 55(12), 1613-1629.

Gerber, H., Malik, A., Solar, G., Sherman, D., Liang, X., Meng, G., Hong, K., Marsters, J., & Ferrara N. (2002). VEGF regulates hematopoietic stem cell survival by an internal autocrine loop mechanism. *Nature*, 417, 954-958.

Gilbert, S. (2000). *Developmental Biology*. 6th edition. Sunderland: Sinauer Associates.

Gobeske, K., Das, S., Bonaguidi, M., Weiss, C., Radulovic, J., Disterhoft, J., & Kessler, J. (2009). BMP Signaling Mediates Effects of Exercise on Hippocampal Neurogenesis and Cognition in Mice. *Public Library of Science One*, 4(10), e7506. doi:10.1371/journal.pone.0007506

Han, Y. & Lefebvre, V. (2008). L-Sox5 and Sox6 drive expression of the aggrecan gene in cartilage by securing binding of Sox9 to a far-upstream enhancer. *Molecular & Cellular Biology*, 28(16), 4999-5013.

Harada, S. & Rodan, G. (2003). Control of osteoblast function and regulation of bone mass. *Nature*, 423, 349-355.

Henriksen, K., Tanko, L., Qvist, P., Delmas, P., Christiansen, C., & Karsdal, M. (2007). Assessment of osteoclast number and function: application in the development of new and improved treatment modalities for bone diseases. *Osteoporosis International*, 18, 681-685.

Higuchi, M., Kato, T., Chen, M., Yako, H., Yoshida, S., Kanno, N., & Kato, Y. (2013). Temporospatial gene expression of Prx1 and Prx2 is involved in morphogenesis of cranial placode-derived tissues through epithelio-mesenchymal interaction during rat embryogenesis. *Cell & Tissue Research*, 353(1), 27-40.

Hines, J., Ju, R., Dutschman, G., Cheng, Y., & Crews, C. (2010). Reversal of TNP-470-induced endothelial cell growth arrest by guanine and guanine nucleosides. *Journal of Pharmacology & Experimental Therapeutics*, 334(3), 729-738.

Holmes, K., Roberts, O., Thomas, A., Cross, M. (2007). Vascular endothelial growth factor receptor-2: Structure, function, intracellular signalling and therapeutic inhibition. *Cellular Signalling*, 19, 2003-2012.

Kashima, T., Dongre, A., Oppermann, U., & Athanasou, N. (2013). Dentine matrix protein 1 (DMP-1) is a marker of bone-forming tumours. *Virchows Archiv The European Journal of Pathology*, 462, 583-591.

Kellermair, J., Redwan, B., Alias, S., Jabkowski, J., Panzenboeck, A., Kellermair, L., Winter, M., Weltermann, A., & Lang, I. (2013). Platelet endothelial cell adhesion molecule 1 deficiency misguides venous thrombus resolution. *Blood*, 122, 3376-3384.

Khan, S. & Lane, J. (2004). The use of recombinant human bone morphogenetic protein-2 (rhBMP-2) in orthopaedic applications. *Expert Opinion on Biological Therapy*, 4(5), 741-748.

Kondo, M., Yamaoka, K., Sonomoto, K., Fukuyo, S., Oshita, K., Okada, Y., & Tanaka, Y. (2013). IL-17 inhibits chondrogenic differentiation of human mesenchymal stem cells. *Public Library of Science One*, 8(11), e79463. doi:10.1371/journal.pone.0079463

Lee, M., Kwon, T., Park, H., Wozney, J., & Ryoo, H. (2003). BMP-2-induced Osterix expression is mediated by Dlx5 but is independent of Runx2. *Biochemical & Biophysical Research Communications*, 309, 689-694.

Leung, V., Gao, B., Leung, K., Melhado, I., Wynn, S., Au, T., Dung, N., Lau, J., Mak, A., Chan, D., & Cheah, K. (2011). SOX9 governs differentiation stage-specific gene expression in growth plate chondrocytes via direct concomitant transactivation and repression. *Public Library of Science Genetics*, 7(11), e1002356. doi:10.1371/journal.pgen.1002356

Lips, P. (2001). Vitamin D Deficiency and Secondary Hyperparathyroidism in the Elderly: Consequences for Bone Loss and Fractures and Therapeutic Implications. *Endocrine Reviews*, 22(4), 477-501.

Liu, R., Schindeler, A., & Little, D. (2010). The potential role of muscle in bone repair. *Journal of Musculoskeletal and Neuronal Interactions*, 10(1), 71-76.

Mackie, E., Ahmed, Y., Tatarczuch, L., Chen, K., & Mirams, M. (2008). Endochondral ossification: How cartilage is converted into bone in the developing skeleton. *The International Journal of Biochemistry & Cell Biology*, 40(1), 46-62.

Maddox, E., Zhan, M., Mundy, G., Drohan, W., & Burgess, W. (2000). Optimizing Human Demineralized Bone Matrix for Clinical Application. *Tissue Engineering*, 6(4), 441-448.

Maltzahn, J., Jones, A., Parks, R., & Rudnicki, M. (2013). Pax7 is critical for the normal function of satellite cells in adult skeletal muscle. *Proceedings of the National Academy of Sciences USA*, 110(41), 16474-16479.

Matsubara, H., Hogan, D., Morgan, E., Mortlock, D., Einhorn, T., & Gerstenfeld, L. (2012). Vascular tissues are a primary source of BMP2 expression during bone formation induced by distraction osteogenesis. *Bone*, 51(1), 168-180.

Mescher, A. (2010). *Junqueira's Basic Histology*. New York: The McGraw-Hill Companies, Inc.

NCI Drug Dictionary. (n.d.). *National Cancer Institute*. Retrieved Jan. 23, 2014, from http://www.cancer.gov/drugdictionary?CdrID=41725

Park, S., Seo, K., So, A., Seo, M., Yu, K., Kang, S., & Kang, K. (2012). SOX2 has a crucial role in the lineage determination and proliferation of mesenchymal stem cells through Dickkopf-1 and c-MYC. *Cell Death & Differentiation*, 19(3), 534-545.

Peng, H., Usas, A., Olshanski, A., Ho, A., Gearhart, B., Cooper, G., & Huard, J. (2005). VEGF Improves, Whereas sFlt1 Inhibits, BMP2-Induced Bone Formation and Bone Healing Through Modulation of Angiogenesis. *Journal of Bone & Mineral Research*, 20(11), 2017-2027.

Physical Fields. (2002). *American Academy of Orthopaedic Surgeons*. Retrieved Jan. 23, 2014, from http://orthoinfo.aaos.org/topic.cfm?topic=A00279

Pietrzak, W., Perns, S., Keyes, J., Woodell-May, J., & McDonald, N. (2005). Demineralized Bone Matrix Graft: A Scientific and Clinical Case Study Assessment. *The Journal of Foot and Ankle Surgery*, 44(5), 345-353.

Pietrzak, W., Woodell-May, J., & McDonald, N. (2006). Assay of bone morphogenetic protein-2, -4, and -7 in human demineralized bone matrix. *The Journal of Craniofacial Surgery*, 17(1), 84-90.

Saito, A., Suzuki, Y., Ogata, S., Ohtsuki, C., & Tanihara, M. (2005). Accelerated bone repair with the use of a synthetic BMP-2-derived peptide and bone-marrow stromal cells. *Journal of Biomedical Materials Research*, 72A(1), 77-82.

Schwaerzer, G., Hiepen, C., Schrewe, H., Nickel, J., Ploeger, F., Sebald, W., Mueller, T., & Knaus, P. (2012). New Insights into the Molecular Mechanism of Multiple Synostoses Syndrome (SYNS): Mutation Within the GDF5 Knuckle Epitope Causes Noggin-Resistance. *Journal of Bone & Mineral Research*, 27(2), 429-442.

Sharma, A., Meyer, F., Hyvonen, M., Best, S., Cameron, R., & Rushton, N. (2012). Osteoinduction by combining bone morphogenetic protein (BMP)-2 with a bioactive novel nanocomposite. *Bone & Joint Research*, 1, 145-151.

Shimozaki, K., Clemenson, G., & Gage, F. (2013). Paired related homeobox protein 1 is a regulator of stemness in adult neural stem/progenitor cells. *The Journal of Neuroscience*, 33(9), 4066-4075.

Smits, P., Li, P., Mandel, J., Zhang, Z., Deng, J., Behringer, R., de Crombrugghe, B., Lefebvre, V. (2001). The Trascription Factors L-Sox5 and Sox6 Are Essential for Cartilage Formation. *Developmental Cell*, 1, 277-290.

Takahashi, K. & Yamanaka, S. (2006). Induction of Pluripotent Stem Cells from Mouse Embryonic and Adult Fibroblast Cultures by Defined Factors. *Cell*, 126, 663-676.

Tomlinson, R., McKenzie, J., Schmieder, A., Wohl, G., Lanza, G., & Silva, M. (2013). Angiogenesis is required for stress fracture healing in rats. *Bone*, 52(1), 212–219.

Tsuji, K., Bandyopadhyay, A., Harfe, B., Cox, K., Kakar, S., Gerstenfeld, L., Einhorn, T., Tabin, C., & Rosen, V. (2006). BMP2 activity, although dispensable for bone formation, is required for the initiation of fracture healing. *Nature Genetics*, 38(12), 1424-1429.

Weber, M., Sotoca, A., Kupfer, P., Guthke, R., & van Zoelen, E. (2013). Dynamic modeling of microRNA regulation during mesenchymal stem cell differentiation. *BioMed Central Systems Biology*, 7, 124.

Wheeler, P. & Batt, M. (2005). Do non-steroidal anti-inflammatory drugs adversely affect stress fracture healing? A short review. *British Journal of Sports Medicine*, 39, 65-59.

Wozney, J. & Rosen, V. (1998). Bone Morphogenetic Protein and Bone Morphogenetic Protein Gene Family in Bone Formation and Repair. *Clinical Orthopaedics & Related Research*, 346, 26-37.

Yang, C., Yang, L., & Cao, X. (2010). Generation of a mouse model with expression of bone morphogenetic protein type II receptor lacking the cytoplasmic domain in osteoblasts. *Annals of the New York Academy of Sciences*, 1192, 286-291.

Yasko, A., Lane, J., Fellinger, E., Rosen, V., Wozney, J., & Wang E. (1992). The healing of segmental bone defects, induced by recombinant human bone morphogenetic protein (rhBMP-2). A radiographic, histological, and biochemical study in rats. *The Journal of Bone & Joint Surgery*, 74(5), 659-670.

Zelzer, E., Mamluk, R., Ferrara, N., Johnson, R., Schipani, E., & Olsen, B. (2003). VEGFA is necessary for chondrocyte survival during bone development. *Development*, 131(9), 2161-2171.

Zeng, R., Chen, Y., Zeng, Z., Liu, X., Liu, R., Qiang, O., & Li, X. (2012). Inhibition of mini-TyrRS-induced angiogenesis response in endothelial cells by VE-cadherin-dependent mini-TrpRS. *Heart Vessels*, 27, 193-201.

CURRICULUM VITAE